(Appeared in *Tectonophysics*, **478**, 3-18, 2009)
DOI: http://dx.doi.org/10.1016/j.tecto.2009.02.018

Detection of aeromagnetic anomaly change associated with volcanic activity: an application of the generalized mis-tie control method

Tadashi Nakatsuka [a], Mitsuru Utsugi [b], Shigeo Okuma [a],
Yoshikazu Tanaka [b], and Takeshi Hashimoto [c]

[a] *Geological Survey of Japan, AIST* (Higashi 1-1-1, Tsukuba 305-8567, Japan)
[b] *Aso Volcanological Laboratory, Kyoto Univ.* (Kawayou 5280-1, Minami-Aso, Kumamoto 869-1404, Japan)
[c] *Institute of Seismology and Volcanology, Hokkaido Univ.* (Kita-10 Nishi-8, Kita-ku, Sapporo 060-0810, Japan)

Received 29 November 2007; revised 12 January 2009; accepted 16 February 2009. Available online 28 February 2009.

Keywords: aeromagnetic anomalies, mis-tie control method, magnetic anomaly change, volcanic activity, Asama Volcano

Abstract

Repeat aeromagnetic surveys may assist in mapping and monitoring long-term changes associated with volcanic activity. However, when dealing with repeat aeromagnetic survey data, the problem of how to extract the real change of magnetic anomalies from a limited set of observations arises, i.e. the problem of spatial aliasing. Recent development of the generalized mis-tie control method for aeromagnetic surveys flown at variable elevations enables us to statistically extract the errors from ambiguous noise sources. This technique can be applied to overcome the spatial alias effect when detecting magnetic anomaly changes between aeromagnetic surveys flown at different times. We successfully apply this technique to Asama Volcano, one of the active volcanoes in Japan, which erupted in 2004. Following the volcanic activity in 2005, we conducted a helicopter-borne aeromagnetic survey, which we compare here to the result from a previous survey flown in 1992. To discuss small changes in magnetic anomalies induced by volcanic activity, it is essential to estimate the accuracy of the reference and the repeat aeromagnetic measurements and the probable errors induced by data processing. In our case, the positioning inaccuracy of the 1992 reference survey was the most serious factor affecting the estimation of the magnetic anomaly change because GPS was still in an early stage at that time. However, our analysis revealed that the magnetic anomaly change over the Asama Volcano area from 1992 to 2005 exceeded the estimated error at three locations, one of which is interpreted as a loss of magnetization induced by volcanic activity. In this study, we suffered from the problem of positioning inaccuracy in the 1992 survey data, and it was important to evaluate its effect when deriving the magnetic anomaly change.

1. Introduction

It is widely believed that magnetic anomalies on active volcanoes change in relation to volcanic activities, especially by thermal demagnetization effects and terrain deformation (e.g., Rikitake and Yokoyama (1955), Hamano *et al.* (1990), Sasai *et al*. (2002), Hurst *et al.* (2004)). Repeat aeromagnetic surveys offer a promising way of analyzing the magnetic effects of volcanic activity.

Continuous ground-based magnetic observations near a volcanic crater or in the active zone can reveal the detailed magnetic effects of volcanic activity (e.g., Tanaka (1993), Sasai *et al.* (2002)). However, volcano-magnetic effects observed from ground-magnetic surveys are generally restricted to small target areas because of the limited spatial distribution of ground stations. On the contrary, repeat aeromagnetic surveys will have significant advantage in the spatial coverage, but their temporal resolution is typically much poorer. Therefore, it is effective to complementally use both methods to monitor the magnetic anomaly change caused by volcanic activity.

In dealing with repeat aeromagnetic survey data, there is first the problem of how to extract the real change of magnetic anomalies from a limited set of repeat observations. Nakatsuka *et al.* (1990) conducted an aeromagnetic survey soon after the beginning of the Izu-Oshima 1986 eruption in Japan and compared it with the magnetic anomaly data collected during the previous 1978 survey. The flying altitude, line direction and line spacing were equivalent, but the locations of survey lines were different between the two surveys. The difference between magnetic anomaly maps (gridded data) derived from the two surveys reached values as high as 300nT. However, after a detailed examination of the reproducibility of magnetic anomalies, Nakatsuka *et al.* (1990) concluded that the difference was mainly caused by the spatial alias effect from the different locations of observation lines (Fig. 1). It is probable that the actual magnetic anomaly pattern in Fig. 1(b) was sampled at open and closed dots in 1978 and 1986 survey, respectively, which produced anomaly maps corresponding to solid and broken lines in Fig. 1(a), respectively.

To study the recent activity of Unzen Volcano, an aeromagnetic survey was conducted in August 1991 (Nakatsuka, 1994). The only previous aeromagnetic data over the study area were collected during the 1981 survey by the New Energy Development Organization, Japan (NEDO), which however had a coarser line spacing. The magnetic anomaly difference after the reduction to a common altitude revealed that the peaks of the difference are distributed in the middle of the NEDO survey lines, and larger differences are in zones of higher magnetic field gradients (Nakatsuka, 1994). This situation suggests that the magnetic anomaly difference is mainly caused by the spatial alias effect from the wider line spacing of the NEDO survey along with the inaccurate positioning data of the 1981 NEDO survey when GPS was still not available.

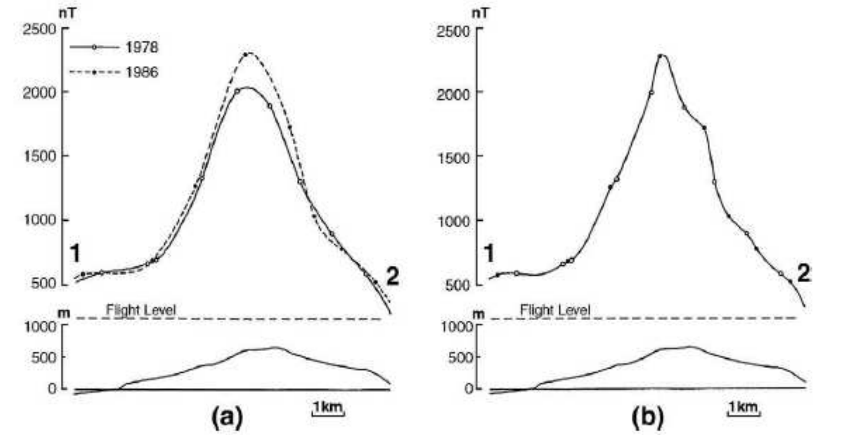

Fig. 1 Magnetic anomaly (top) and topography (bottom) profile along E-W section across the magnetic anomaly peak of Izu-Oshima Volcano. Dots and small open circles correspond to the 1986 and 1978 survey lines (in N-S direction). The apparent difference between broken and solid lines on the left (a), interpolated from each survey, was interpreted as the spatial alias effect as shown on the right (b) (after Nakatsuka *et al.*, 1990).

More recently, Hurst *et al.* (2004) reported their comprehensive study on the thermo-magnetic effect in White Island, New Zealand, and they also discussed the necessity of close line spacing to overcome errors from the interpolation process. The Hydrographic Department, Maritime Safety Agency, Japan carried out aeromagnetic surveys of Miyake-jima Volcano in 1987, 1999, and 2001, covering the Miyake-jima 2000 eruption, and Ueda (2006) discussed the subsurface magnetic structure model of the volcano. However, the line spacing was too sparse to discuss the change of magnetic anomaly distribution, and they did not mention the reproducibility of magnetic anomalies. After Usu Volcano began to erupt in March 2000, the Geological Survey of Japan (Okuma *et al.*, 2001, 2003) carried out an airborne geophysical survey in the Usu area as a part of the national emergency program of monitoring the volcanic activity of Usu. They discussed the geologic structure of Usu Volcano, however, the temporal magnetic anomaly change could not be addressed because of the lack of a high-resolution aeromagnetic survey before the eruption.

When we try to extract the magnetic anomaly change from the data of repeat aeromagnetic surveys, we must consider the reproducibility of magnetic anomalies and the spatial alias effect because the survey line tracks cannot be the same. Therefore, it is important to obtain data with sufficiently close line spacing. In reality, however, the reference survey typically features a non-ideal survey design because of the unknown scale and location of future volcanic activity. Hence, in most cases we cannot avoid handling aeromagnetic datasets that have insufficient spatial resolution and variable accuracies. To overcome these difficulties, Nakatsuka and Okuma (2006b) suggested a new method. They developed a method of crossover analysis applicable to helicopter-borne aeromagnetic surveys in rugged terrain areas and called it the “generalized mis-tie control method”. The method statistically estimates some noise field contamination in the data by extending the altitude reduction procedure to take the mis-tie adjustment parameters into account. If we consider aeromagnetic data collected at two different times, the survey line direction of which is perpendicular to each other, this method will provide an estimation of the magnetic anomaly change between these two times. Although the method was first developed for crossover points of two sets horizontal trajectories perpendicular each other, the selection of crossover points as control points is not essential mathematically, as there is still altitude difference between two crossover lines. The method can be applied to any selected control points, as is discussed in this paper where the perpendicular survey arrangement could not be realized.

In 2004-2005, eruptive activity took place at Asama Volcano, and we had an opportunity to conduct an aeromagnetic survey in 2005 with a line spacing of 250 m. As for the reference data, we had a high-resolution aeromagnetic survey (with an average line spacing of 150 m) performed in 1992 by the Geological Survey of Japan (Okuma et al., 2005). In this paper, we deal with the comparison of these two aeromagnetic surveys over Asama Volcano, and discuss the application of the generalized mis-tie control method to the problem of estimating the magnetic anomaly change induced by volcanic activity. Even in the case of relatively tight survey line spacing, the spatial alias effect is still the main issue to address, which we achieve by applying the generalized mis-tie control method of Nakatsuka and Okuma (2006b). A significant additional factor to be considered is the accuracy of the magnetic anomaly distribution derived from each survey. When doing so we must analyze two kinds of error sources, magnetic field measurement and positioning errors. As we discussed in our paper, the positioning error encountered in the older (reference) survey may be highly significant especially for the purpose of detecting the magnetic anomaly change.

We know that careful inspection to the errors is essential to derive magnetic anomaly change between repeat aeromagnetic surveys. So we discuss various probable error sources, and only the parts exceeding error ceiling are considered valid. In reality, the effect of positioning error in the area of high magnetic anomaly gradients was the crucial problem. The magnetic anomaly gradient, however, is dependent on the position. As we know the actual magnetic field distribution, we can evaluate the error level at each observation point related to the position inaccuracy, as is described in this paper.

2. Generalized mis-tie control for an aeromagnetic survey at varying elevations

Crossover analysis is an efficient technique of improving survey accuracy, which has been widely adopted in fixed-wing surveys flown at constant barometric altitudes. This technique is based on the fact that a magnetic anomaly at the same point should be same. However, in rugged terrain areas, real survey lines are unlikely to be on a plane, and hence profile lines and tie lines do not intersect in an ideal 2D configuration. Therefore, we must take the altitude differences into account to estimate the crossover mismatch, and we want to estimate the mismatch parameters together with equivalent source parameters for altitude reduction.

We start with the equivalent source technique of altitude reduction (Nakatsuka and Okuma, 2006a).

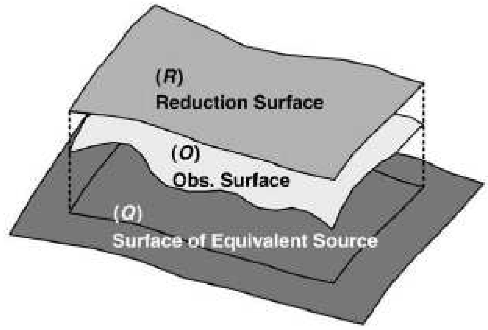

Fig. 2 Scheme of the altitude reduction process by an equivalent source.

Now we consider the problem (Fig. 2) of reducing the magnetic anomaly observed on an undulated surface O into a smooth surface R, assuming the source is distributed on Q.

The basic formula of equivalent source analysis is given by

$$F(\boldsymbol{p}) = \int_Q A(\boldsymbol{p},\boldsymbol{q})\, S(\boldsymbol{q})\, ds \,, \qquad (1)$$

where $S(\boldsymbol{q})$ is the equivalent source distribution at the source location $\boldsymbol{q}$ on the infinite (or closed) surface Q, $F(\boldsymbol{p})$ is the (total field) magnetic anomaly at observation point $\boldsymbol{p}$ above (or outside) Q, and $A(\boldsymbol{p},\boldsymbol{q})$ is the harmonic function combining $F(\boldsymbol{p})$ with $S(\boldsymbol{q})$. Equivalent source distribution $S(\boldsymbol{q})$ can be given from the observation $F(\boldsymbol{p})$ as a solution of the inverse problem of Eq (1).

Once the Eq (1) is solved, the reduction to any surface is calculated with the same Eq (1). In the numerical calculation, Eq (1) is replaced with a summation over a finite source area, and the problem is reduced to solving simultaneous linear equations with vector/matrix notation,

$$\begin{pmatrix} \boldsymbol{F} \end{pmatrix} = \begin{pmatrix} \quad \mathbf{A} \quad \end{pmatrix} \begin{pmatrix} \boldsymbol{S} \end{pmatrix} \qquad \left[F_x = \sum_i A_{ix} S_i \right]. \qquad (2)$$

The source area is selected wider than the observation region to avoid the numerical edge effect, as suggested by Nakatsuka and Okuma (2006a). Although the problem is usually underdetermined, the conjugate gradient (CG) method can give a favorable solution of the norm minimum (Nakatsuka, 1995).

Next, we take the effect of crossover mismatch into account. The crossover differences have traditionally been attributed to the positional error and/or magnetic level shifts. The positional data acquired from recent GPS systems are quite accurate (typically a few tens centimeters accuracy in an airborne survey with differential post-processing), and hence the crossover differences mostly originate from the errors in the magnetic field data. In the mis-tie control method, the correction for magnetic field data is defined as a linear combination of misfit $\boldsymbol{E}$ at crossover points. Contrary to the traditional process, we cannot know misfit $\boldsymbol{E}$ directly because of the altitude difference. But, we can combine this effect with the equivalent source analysis,

$$\left(\boldsymbol{F} \right) = \left(\mathbf{A} \middle| \mathbf{B} \right) \left(\frac{\boldsymbol{S}}{\boldsymbol{E}} \right)$$

$$\left[F_x = \sum_i A_{ix} S_i + \sum_j B_{jx} E_j \right], \qquad (3)$$

where $\mathbf{B}$ is the matrix of contribution factors of magnetic level shifts to the observation $\boldsymbol{F}$. Here, $\mathbf{A}$ and $\mathbf{B}$ constitutes a combined matrix to be applied to the combined vector of $\boldsymbol{S}$ and $\boldsymbol{E}$. The combined equation is still in the form of simultaneous linear equations, and the CG method can be applied to obtain the minimum norm solution. In the case of general mis-tie control against ambiguous noise source, the crossover difference can originate from both data of corresponding lines, i.e., two parameters collaborate to explain one crossover difference. In our case, however, as we expect the noise source is the magnetic anomaly change after the reference survey, only one parameter on the repeat survey line is considered.

We developed a simple model to test the ability of the generalized mis-tie control method in deriving the magnetic anomaly change between a reference and a repeat survey. Figure 3 consists of six panels, each covering a 6km×6km area, and the anomalous source bodies are considered as shown in panel A. We assume the observation was made along 12 N-S trending survey lines (panel B) for the reference survey when two source bodies 1 and 2 exist, and an additional source 3 exists for the repeat survey flown along 12 E-W oriented lines (panel B). The source cubic bodies 1 and 2 with magnetization of 2 A/m have an extent of 1 km^3 situated at the top depths of the sea level, and the additional source 3 is a 500m×500m×800m block of negative magnetization –2 A/m with a top depth of 200 m under the sea level. The contours in panel B indicate the altitude of the common reduction surface (smoothed from observation altitudes), on which the source 3 effect in panel A is calculated. From the procedure of the generalized mis-tie control, the magnetic anomaly change was estimated as C, which is an adequate approximation to the ideal pattern A. On the other hand,

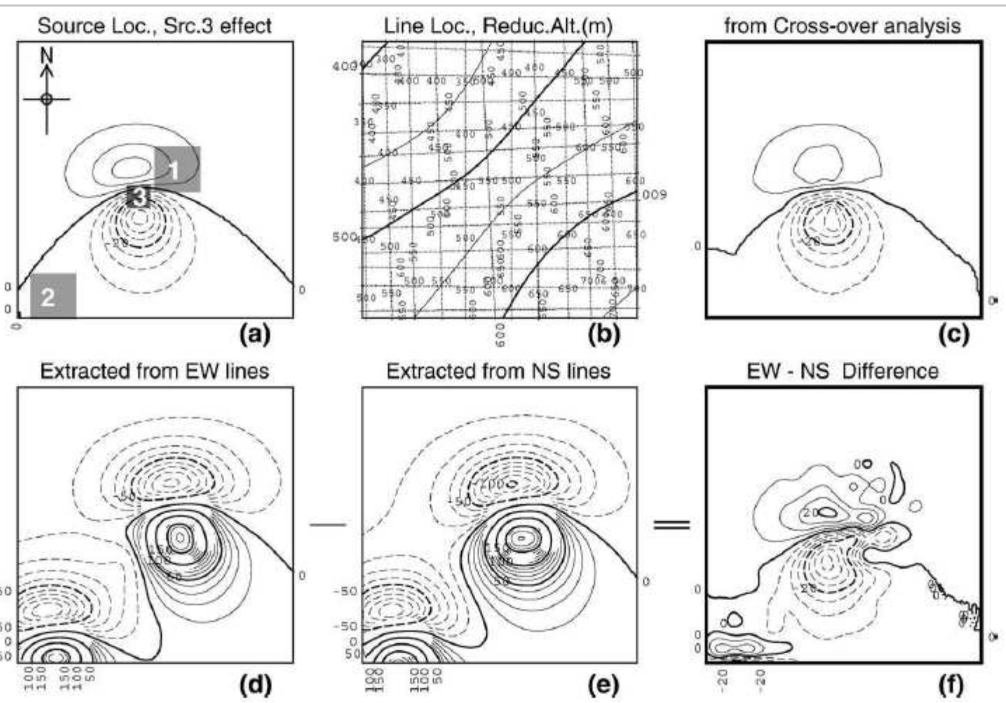

Fig. 3 Synthetic model example showing how a magnetic anomaly change induced by a change in volcanic sources can be revealed by the generalized mis-tie control method applied to repeat aeromagnetic surveys. The source model is shown in A, where a negative source 3 is present only for idealized E-W oriented flight lines. Contours in A represents the effect of source 3 on a smooth reduction surface, shown as contours in panel B. Note that 12 N-S lines and 12 E-W lines (with the respective altitude values) were assumed to represent the two aeromagnetic surveys flown at different times. From the generalized mis-tie control method, the magnetic anomaly change was estimated as C, which is an adequate approximation to the ideal pattern A. On the other hand, the difference D between the simple reductions E and F to the common surface, calculated from E-W lines and N-S lines, respectively, reveals a contamination of noise because of the spatial alias effect. The contour intervals are 10 nT for A, E and F, 5 nT for C and D, and 50 m for B.

the simple reductions to the common surface were calculated as E from E-W lines, and F from N-S lines. Although the difference D between E and F is another estimate of the magnetic anomaly change, D is contaminated with noise because of the spatial alias effect. This result indicates that the line spacing was insufficient for a conventional method to extract the magnetic anomaly change of source 3. If we obtained higher-resolution data with half the line spacing, then the magnetic anomaly change could also be extracted reasonably from the difference between two simple reductions to a common surface (Nakatsuka and Okuma, 2006b).

Now we will apply this method of generalized mis-tie control to actual survey data.

3. Asama Volcano and aeromagnetic survey data

Mt. Asama is one of the active volcanoes in Japan, located at the junction of two volcanic fronts, Central Japan (Fig. 4). The summit elevation is 2568 m near Kama-yama crater, which is the center of recent activities with Vulcanian to Strombolian eruptions. Asama Volcano is a composite volcano made up of three consecutive volcanic edifices (Aramaki, 1993). During the first Kurofu-yama stage, repeated eruptions of lava flows and pyroclastics of andesite formed a large conic edifice, eastern half of which was later destroyed by a large-scale collapse around 20,000 years ago. In the next stage, the Hotoke-iwa stage, that occurred around 14,000-11,000 years BP, dacite and rhyolitic magmas erupted to form a gently sloped lava cone and many pumiceous pyroclastic flows. Several thousand years ago, the Maekake-yama stage activity of pyroxene andesite started to build a stratocone atop the older edifice.

Two major eruptive activities of Asama Volcano in

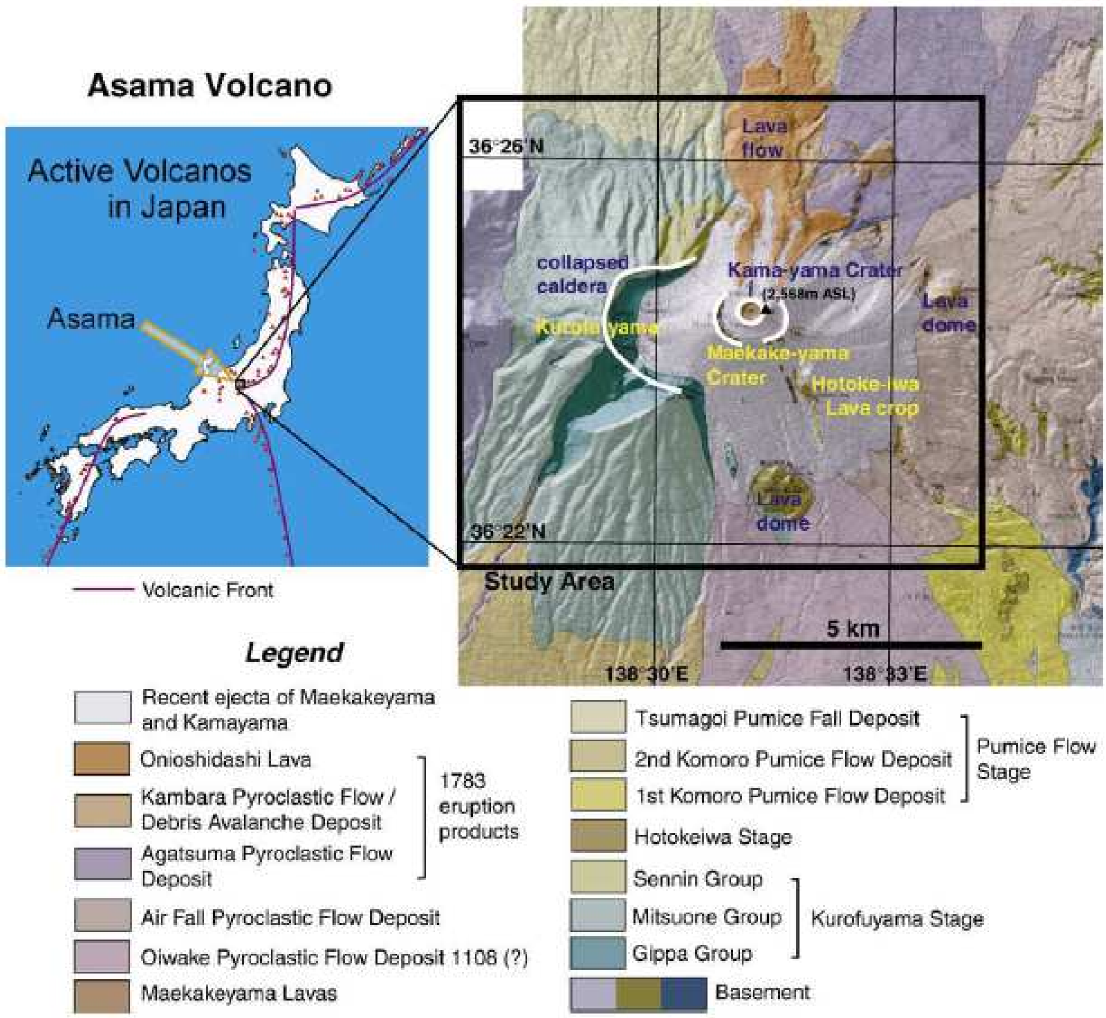

Fig. 4 Location and geology of Asama Volcano. The geology after Aramaki (1993) is shown on the shaded relief of the topography with some key features of the volcano. The thick rectangle is the range of our aeromagnetic study area. Part of a geologic map image in the Database of Japanese Active Volcanoes (http://riodb02.ibase.aist.go.jp/db099/) by the Geological Survey of Japan, AIST was used to prepare this illustration.

1108 and 1783 are known historically and both produced extensive pyroclastic flow deposits and lava flows (Aramaki, 1993). A violent explosion in 1783 produced a peculiar type of pyroclastic flow containing many essential blocks. Those blocks plowed soft early-stage deposits to form a debris avalanche, which destroyed several villages and killed several hundred people. The eruptive activity was high from the end of the 19th century until 1961, and today's summit Kama-yama grew from inside the Maekake-yama crater. Since then, major eruptive activity took place only in 1973 and 2004.

In September-November 2004, several explosive eruptions took place at the summit Kama-yama crater. After this activity, the Asama Volcano EM Field Experiment Group had an opportunity to conduct a helicopter-borne aeromagnetic survey in October 2005 as part of a strategic plan to investigate the volcanic activity and the structure of the volcano. We used an optically pumped Cesium magnetometer and two GPS receivers in the air, the magnetometer and one GPS receiver were installed in a bird, and the other GPS receiver was on board for the primary purpose of navigation. Another set of an Overhauser magnetometer and a GPS receiver was operated at a ground base station (the location is marked in Fig. 5) in order to facilitate geomagnetic diurnal correction and post-flight differential GPS positioning. The flying altitude was 2000-3200 m above sea-level or 250-1300 m above the ground, and average line spacing was 250 m. Although the differential processing for GPS was not fully available because of different condition of open-sky between the two locations of rover and base GPS receivers, real-time positional data of the on-board GPS were available to fix all positions of the survey tracks with an accuracy of a few meters both in horizontal and vertical directions.

As for the reference data, we had a high-resolution helicopter survey flown in 1992 by the Geological Survey of Japan (Okuma *et al*., 2005). The magnetic field measurements in the air and on the ground were made using proton precession magnetometers, and the survey lines were arranged at a horizontal spacing of 150 m with a flying altitude of 200 m above terrain (i.e. much lower than 2005 survey). The location of ground base station is marked in Fig. 6. In this survey, the GPS system was first used in an aeromagnetic survey in Japan, when the utilization techniques for GPS were just under development. Hence the positional accuracy was not very high because of the signal condition, military degrading of radio signals, and lack of differential processing. As the altitude data given by GPS were considered erroneous, the combination of a laser altimeter and barometric altimeter was used to fix altitudes. Overall maximum positioning error was

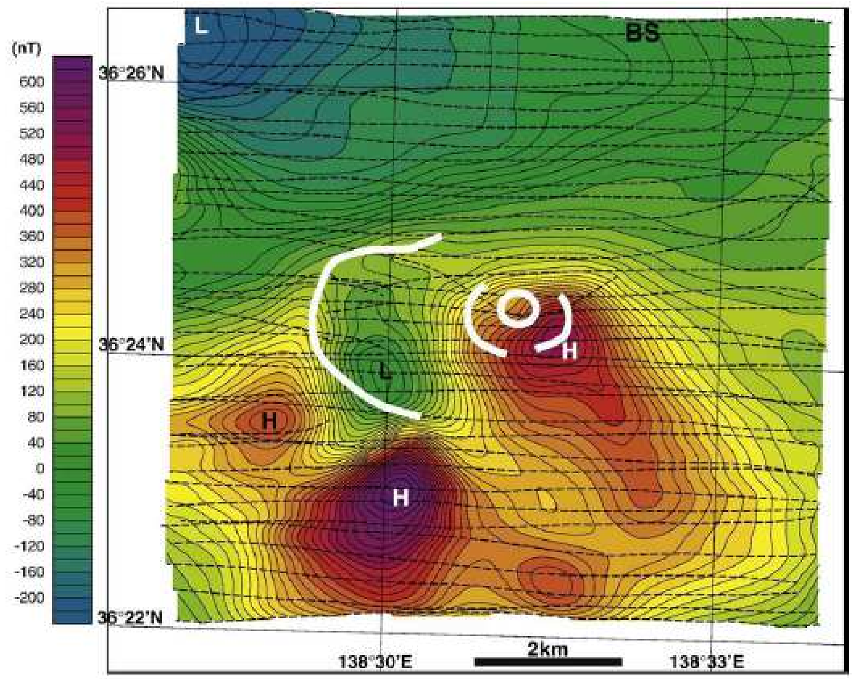

Fig. 5 Aeromagnetic anomalies derived from 2005 survey data on a smooth reduction surface (2100-3000 m ASL). Contour interval is 20 nT. "BS" indicates the location of the ground base station where the geomagnetic and GPS observations were performed for the diurnal correction and the GPS differential post-processing. Broken lines indicate the aeromagnetic survey line paths in all the maps. Thick white curves are the caldera and crater rims in this and the following figures.

estimated to be 60 meters in horizontal (Okuma *et al.*, 2005), while the error in altitudes was considered to be within about 5 meters.

Each survey dataset was processed to map the magnetic anomalies after removing the IGRF-10 model (Maus and Macmillan, 2005) and the diurnal variation observed at the base station. Figures 5 and 6 are the result of the altitude reduction to a smooth surface using the equivalent source technique (Nakatsuka and Okuma, 2006a) applied to the 2005 and 1992 survey data

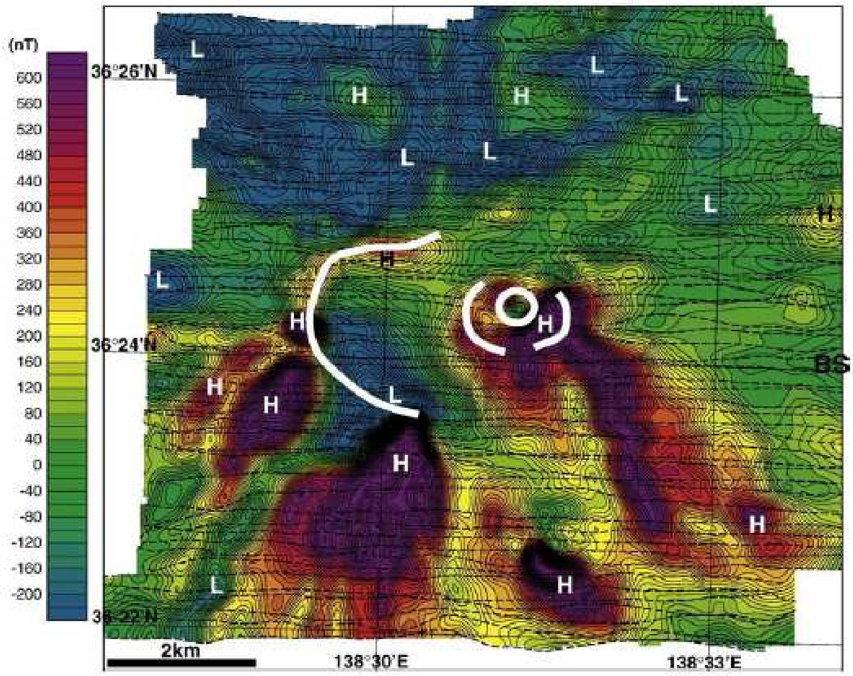

Fig. 6 Aeromagnetic anomalies derived from 1992 survey data on a smooth reduction surface (1300-2650 m ASL). Contour interval is 20 nT. "BS" indicates the location of geomagnetic base station for the diurnal correction in 1992 survey.

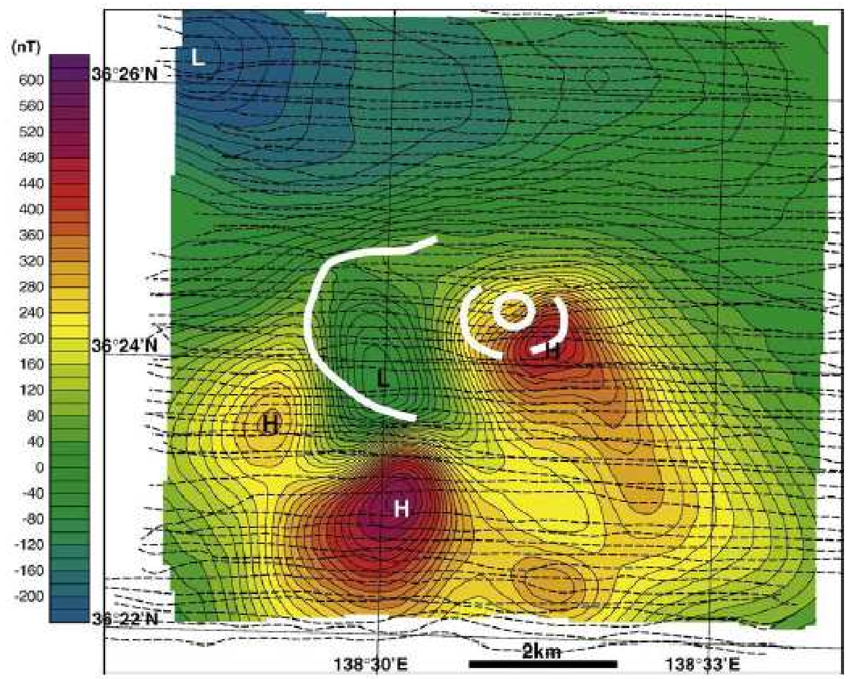

Fig. 7 Aeromagnetic anomalies derived from 1992 survey data after reduction to the surface of 2005 survey altitude (same as in Fig. 5). Contour interval is 20 nT.

respectively. The original observational data and the process parameters of the altitude reduction are given in Appendix. Because the observation altitudes between the two surveys differ considerably, the appearance of magnetic anomalies is also different, as expected. To compare magnetic anomalies at different times, anomaly distributions must therefore be first reduced to a common surface. As the downward reduction process is usually ill-conditioned, the 1992 data of lower altitude were reduced to the altitude of the 2005 survey. This reduction process includes only forward calculation, as the equivalent source model in deriving Fig. 6 was also available for the reduction to a higher reduction surface. The result is shown in Fig. 7, which revealed a more similar anomaly pattern with respect to Fig. 5.

As a first step we subtracted the reduced anomaly pattern (Fig. 7) from the data of the new survey (Fig. 5). Figure 8 is the result of this simple subtraction. Here it should be noted that the altitude reduction process for data of a limited range inevitably includes edge effects. The area inside the thick blue pentagon is the rough range of confidence, where edge effects related to the altitude reduction process we applied are minimal.

4. Application of generalized mis-tie control

Figure 8 contains several magnetic anomaly patterns, which are clearly aligned along the survey flight lines, suggesting that these are residual errors, that may hinder recognition of magnetic anomaly change related to volcanic activity. It is probable that the poorer resolution in the direction across survey lines might cause this kind of difference pattern as a spatial alias effect. Due to this error, we cannot be confident that the three major patterns of change, the decrease *C* in the central area and increases in the northeastern side *N* and southwest *S* are real without further processing. Hence we apply the generalized mis-tie control method described in the previous section. In our case, however, the survey lines are in the E-W direction for both surveys. The actual crossings of horizontal trajectories occur only occasionally and they are distributed unevenly. It is not adequate to pick up only these crossover points for the purpose of mis-tie control. Mathematically, the control points are not necessarily the crossover points of horizontal trajectories, and we may select arbitrary points for the control points. We selected control points at a nearly constant interval of 250 m along the 2005 survey lines.

The result is mapped in Fig. 9, which is drawn from the data of 1090 control points represented by small circles. Since there was a gentle trend dipping north that can be seen in Fig. 8, a linear trend of about 7 nT/km

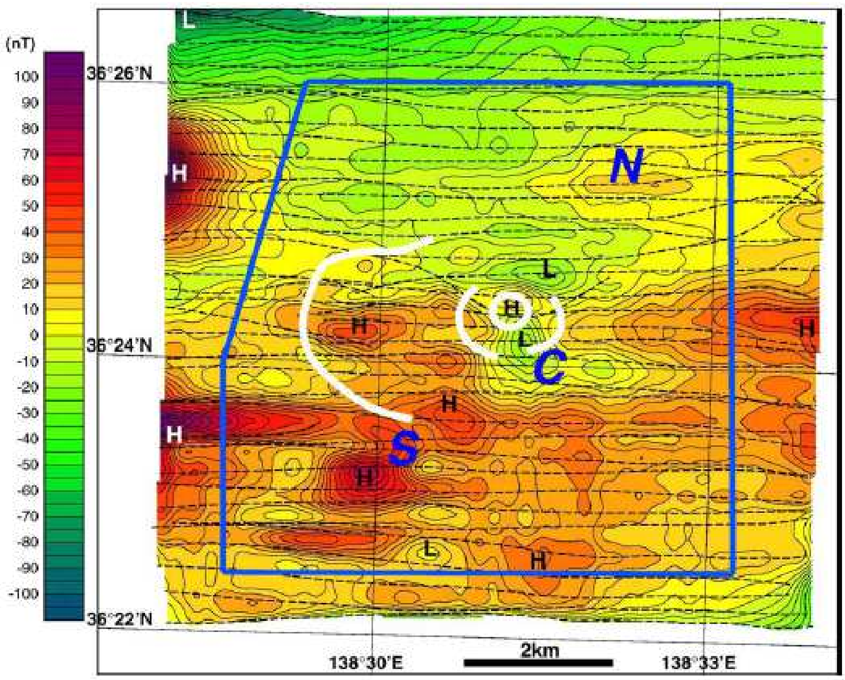

Fig. 8 Simple difference between aeromagnetic anomalies of Figs. 5 and 7, which is a poor estimation of magnetic anomaly change between 1992 and 2005. Contour interval is 5 nT, one fourth of those in previous figures. Aeromagnetic survey lines (broken lines) are shown only for the 2005 survey. The area inside the thick blue pentagon is the rough range of confidence, where edge effects related to the altitude reduction process we applied are minimal.

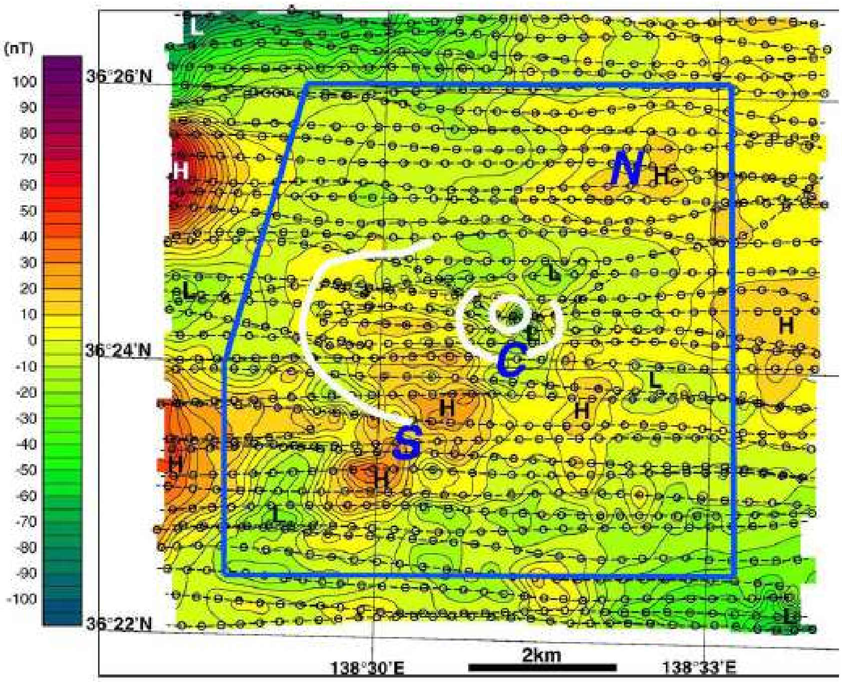

Fig. 9　Estimation of aeromagnetic anomaly change between 1992 and 2005 by the generalized mis-tie control method. Contour interval is 5 nT.　Anomaly values are calculated at the altitude of the higher elevation survey lines flown in 2005.　Circles indicate the locations of control points used in the generalized mis-tie control method.

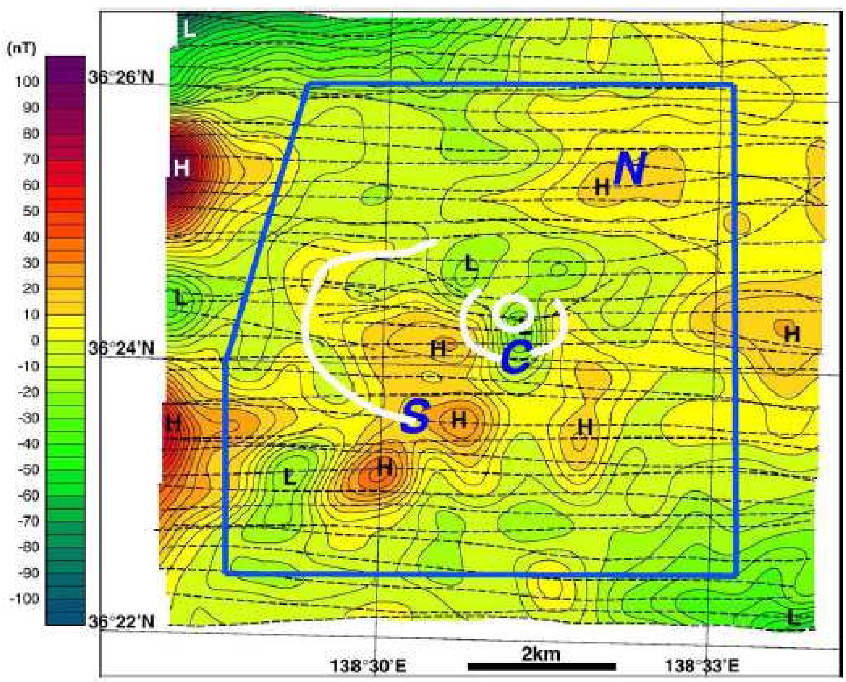

Fig. 10　Aeromagnetic anomaly change calculated on the smooth reduction surface used also in Fig. 8. Contour interval is 5 nT.

has been removed. The reason for this trend is that the IGRF correction used to obtain the residual aeromagnetic anomalies from both surveys has a secular change, which may not be adequately predicted for a localized region, such as our study area.　Also it is possible that the offset between the two surveys may be affected by the extra-terrestrial source effect such as related to solar activity. The reference altitudes in Fig. 9 are those on actual flight lines, that is, the map shows the distribution on an undulated and distorted surface.　Therefore, we tried to reduce this pattern onto a smooth surface (same as in Figs. 5 and 7). The number of data points (1090) may be insufficient for such a reduction, and we must accept that some distortion will remain. Nevertheless, we obtained a distribution that maintains the main magnetic features (Fig. 10).

In Figs. 9 and 10, there are no peculiar patterns compared to Fig. 8 because the adoption of the generalized mis-tie control method was effective in mitigating the spatial alias effect especially in the direction across the survey lines. In our case, Fig. 8 did show the three major patterns of magnetic change despite the presence of residual corrugation of the signal. However, if the spatial alias effect had been more significant, it is likely that even the major magnetic change patterns might have been concealed.

5. Magnetic anomaly change between two surveys

Pattern *C* corresponds to a relative decrease in magnetic anomaly intensity, and overlies the area of the Kama-yama crater, the eruptive vent of the 2004 volcanic activity. Area *S* features a relative increase of magnetic anomaly, and corresponds to a broad area located to the south to southwest of the volcano. The area *N* of relative magnetic increase corresponds to the head zone of the 1783 activity, where a thick formation of lava or welded deposits is expected. The magnetic anomaly decrease (*C*) seems to be interpreted reasonably as arising from thermal demagnetization of rocks and/or a loss of remanent bulk magnetization by the 2004 explosive eruption. On the other hand, in the areas of magnetic anomaly increase (*S* and *N*) we have no evidence of any process potentially causing it. As the anomaly change is the difference between two surveys separated by a 13 years interval, there is a possibility that the volcanic rocks may have acquired a slightly stronger magnetization as a result of the quiet period of volcanic activity. Actually, the magnetic anomaly increase *S* is situated as surrounding the highest magnetic anomaly peak in Fig. 5 (or in Fig. 6), and *N* is on a gentle ridge pattern (swelling of contour lines) of the magnetic anomaly in Fig. 5, which corresponds to the NE-SW trending high magnetic anomaly in Fig. 6. However, a more detailed examination of the accuracy of the predicted change is required, and especially the effect of the positioning error must be addressed.

6. Errors estimation

Before we proceed to the positioning error, we check the errors in the magnetic field measurement and its corrections. The optically pumped and proton precession magnetometers are very stable equipment, and an accuracy much better than 1 nT is attained. Hence the reproducibility of magnetic field values is mainly restricted by artificial noise sources and the correction for diurnal variations. The error in the diurnal correction is small in the low to mid latitude areas if the ground station is near the survey area, unless strong magnetic storms occur (we survey in magnetically quiet days). We are confident that this error in our data is less than 1 nT. One artificial noise source is the aircraft itself having its own magnetization. But, as the sensor of the airborne magnetometer was towed in a bird configuration with a 40 m long cable, its noise level is within 1 nT. Another artificial noise source is the effect of an electric railroad powered by DC, which generates a magnetic field disturbance. The difference in this disturbance between the airborne magnetic sensor and the magnetic base station becomes the error. About 10 km south of the survey area, there was the main line of a DC powered railroad in 1992, which was replaced by a bullet train line powered by AC in 1997. From a preliminary ground survey, we could expect the magnetic field observation in the air and at the ground magnetic station in 1992 was contaminated with noise of a few nanotesla at the maximum. From the above considerations, we can assume the maximum error of magnetic field observations is less than 5nT for the comparison of 1992 and 2005 aeromagnetic data.

There is also another problem of the secular change of the normal field, which causes an apparent change of the magnetic total field anomaly (Hashimoto, 2006). We estimated this effect on our observations, by assuming that the magnetic anomalies are caused by an equivalent source with only remanent magnetization, as it is known that the magnetization of volcanic rocks generally have Königsberger (Q_n) ratio higher than unity, i.e., natural remanent component exceeds the induced one (e.g., Nagata (1943), Nagata and Uyeda (1961)). As for the direction of the IGRF magnetic field, the inclination increased by 0.3 degree and declination decreased by 0.1 degree from 1992 to 2005, and this secular variation is almost the same as the actual observation at the Kakioka Magnetic Observatory (150 km east of Asama). Figure 11(a) is the result of this estimation with a maximum value less than 3nT excluding the southernmost part where the edge effect of the calculation dominates. A similar estimation can also be done for the induced magnetization. When considering the induced magnetization source, we have to take the secular change of earth's magnetic field intensity into account. The secular change of the intensity between 1992 and 2005 is estimated from IGRF-10 model to be 1/500 increase of the magnitude. The effect of the secular change of the ambient field (including the direction change and the intensity increase) was thus estimated, as is shown in Fig. 11(b). As the magnetic anomaly pattern revealed in Fig. 10 is different and the amplitudes are larger, the effect of the secular change of the normal field is considered to be minor.

As the positioning accuracy of the older survey (Okuma *et al*., 2005) is inferior to today's standard, it is important to estimate the effect of the positioning error for the 1992 survey. Positioning accuracy is particularly relevant in volcanic areas, since these regions typically feature high-magnetic gradients, and hence even small mislocation errors can translate into large differences in magnetic anomalies detected by the repeat aeromagnetic survey. However, it is not a straightforward problem to evaluate the error of the magnetic field value at a specified point caused by the inaccuracy of a position fix. The effect of the positioning error on the magnetic anomalies can be divided into two parts: (1) a misplacement of a magnetic anomaly pattern as expected from a uniform positioning error vector; and (2) a distortion of a magnetic anomaly pattern caused by the scattering of positioning error vectors. In our case of dealing with the altitude reduction, the dominant contribution comes from the observational data within a limited horizontal distance range, because the effect of equivalent sources decreases rapidly as the source's distance to the observer increases. If the positioning error is uniform within this range, we may consider only the former (1). Otherwise we must consider both. The effect of the former (1) is estimated as the multiplication of the positional error distance by the horizontal gradient of the magnetic field distribution. In our case when examining the magnetic anomaly change shown in Fig. 9, the magnetic anomaly pattern from the 2005 survey before the IGRF subtraction can be used to calculate the gradient. On the other hand, the effect of the latter (2) is highly dependent on the survey line layout, wavelength character of magnetic anomalies, and randomness of error scattering. Therefore, we used a simulation technique to estimate the distortion of a magnetic anomaly pattern. The position of each data point of the 1992 survey was shifted by a random value within a maximum error distance, and the same process for deriving the Fig. 7 map was applied to obtain a magnetic anomaly distribution contaminated with the effect of (2). As the difference between this result and data of Fig. 7 reveals only one case of probable error estimations, we repeated the same procedure ten times

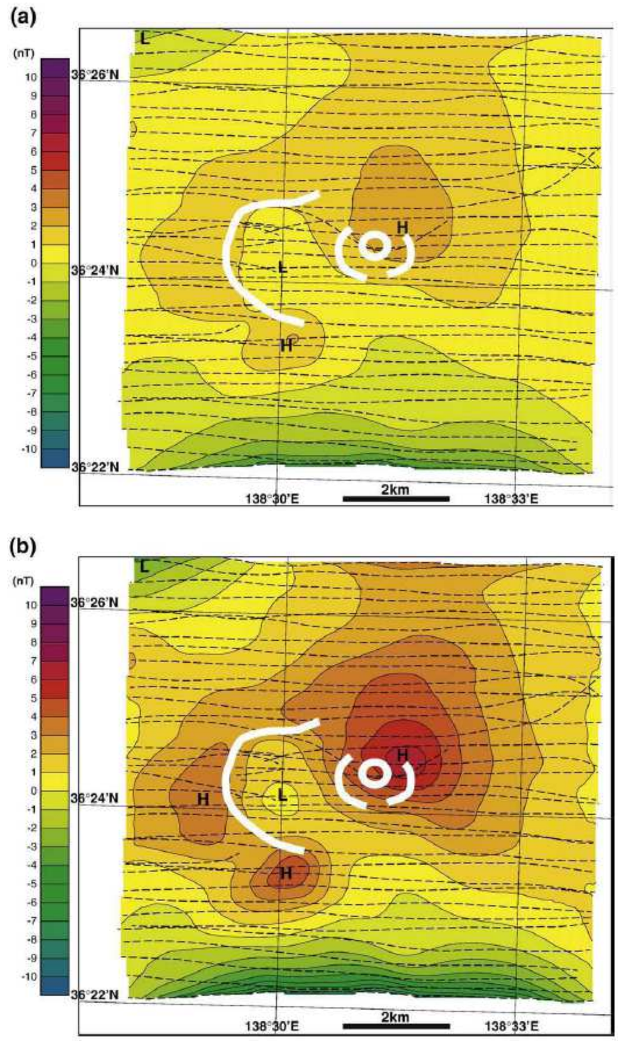

Fig. 11 The effect of secular change of the normal field between 1992 and 2005, as estimated by equivalent source analyses (a) with remanent magnetization only, and (b) with induced magnetization only. Contour interval is 1 nT.

and calculated the root mean square value for each point on the reduction surface to map the distribution.

Figure 12 shows the result of the above calculation for the maximum position error of 60 m, as was estimated for the 1992 survey (Okuma *et al*., 2005). This includes both effects (1) and (2) for the total positioning error, with a peak value of 61 nT. Although this calculation is the error estimation at the maximum, the peak value exceeds the range (–25 nT to +35 nT) of the estimated magnetic anomaly change. That is, extensive parts of Fig. 10 are proven not to be very reliable, and only some values exceeding the range in Fig. 12 should be trusted. As the altitude reduction process from 1992 survey altitude to that of 2005 is a kind of upward continuation filtering, we are fortunate that the shorter wavelength components are smoothed out even for the effect of positioning errors. And we got the result that

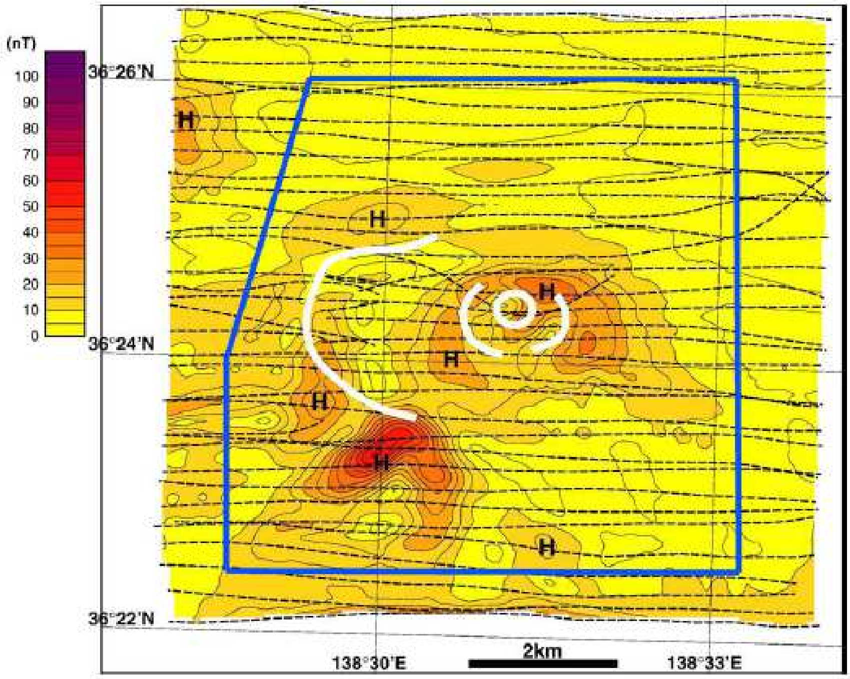

Fig. 12 The effect of the maximum positional error of 60 m in 1992 data, derived as a sum of the effect of (1) misplacement of magnetic anomaly pattern and (2) distortion. Anomaly values are calculated on the common reduction surface, on which magnetic anomaly change between 1992 and 2005 is imaged (i.e., as seen in Figs. 8 and 10). The contour interval is 5 nT.

the misplacement term (1) exceeds the distortion term (2), although we took both into account.

In order to visualize the reliable values for the magnetic anomaly change, the values of estimated mismatch at the control points in Fig. 9 were subtracted by the amount corresponding to Fig. 12. These values were processed again for altitude reduction to the common smooth surface. The final result is given in Fig. 13, in which the area of anomalous values less than 5nT is displayed in white, indicating it is within the maximum error range of the magnetic field observation.

7. Discussion

In Fig. 13, it is easy to recognize that the three major magnetic change patterns *C*, *N* and *S* still exist, which implies that these magnetic anomaly changes actually occurred during the 13-year time interval between the aeromagnetic surveys. Among them, the pattern of the magnetic anomaly increase *S* is considerably different in appearance compared to Fig. 9, probably because of the high magnetic field gradient. The above visualization process has a characteristic that only the area of a smaller expected error is emphasized, and this may distort the real distribution. As the negative zones in the northwest and southeast parts of the blue pentagon are connected to the outer anomalies of the larger edge effect, they are interpreted as the occasional remainder of the edge effect. There are several other small areas of magnetic anomaly change in Fig. 13, but we interpret them as caused by the occasional overlap of another type of error such as the altitude reduction process for a large altitude distance or against a smaller number of data points.

As mentioned before, the magnetic anomaly decrease *C* is interpreted as the result of demagnetization by the 2004 volcanic activity. Okuma *et al*. (2005) estimated the average magnetization of Mt. Asama to be 2.2 A/m from the terrain model matching. The peak magnetic anomaly change of –15 nT to –30 nT can be accounted for by a loss of 2 A/m magnetization of a sphere model with a radius of 160 m to 200 m and placed at a depth of 250 m below the Kama-yama crater rim. This scale of transition is likely for this eruption, although the shape of the magnetization loss may be different compared to the modeled equivalent source one. Actually, the Geographical Survey Institute, Japan (2004 press release) depicted a movement of the bottom level of Kama-yama crater and an alternation of vent materials (estimated volume of exceeding 3×10^6 m^3) from the visual and SAR (Synthetic Aperture Radar) observation in early stage of the activity in 2004, and also from gravimetric observation Ueki *et al*. (2005) suggested a magma movement of the order of 10^7 tonnes. For the magnetic anomaly increases *N* and *S*, the extensions of

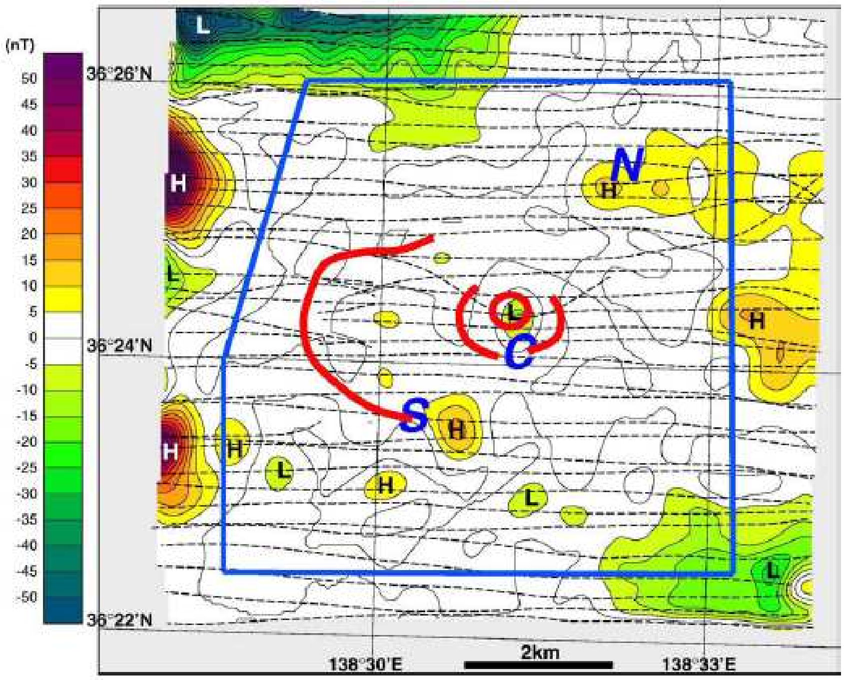

Fig. 13 Estimated magnetic anomaly change between 1992 and 2005 exceeding the expected maximum error from the positioning inaccuracy of the 1992 survey data. Contour interval is 5nT. The areas with values less than 5 nT are shown in white, which indicates that the value is within the error level derived from the correction of the magnetic field observation. The locations of caldera/crater rims are shown by thick red curves.

them are not clear because of the ambiguity as discussed above, and we have no indication of any process causing it. However, it is possible that a large sector of a volcanic edifice acquired slightly stronger magnetization in the course of a quiet period of volcanic activity.

In this study, we suffered from the problem of positioning inaccuracy in the 1992 survey data, and it was important to evaluate its effect when deriving the magnetic anomaly change, especially in volcanic areas where a large magnetic gradient is expected. Since the GPS positioning technique has developed considerably in recent years, a positional accuracy of a few meters in mobile observations is easily attained in real-time, and 5-10 cm accuracy is possible for fully processed kinematic GPS data under a good condition of the radio signal and satellite configuration. Notably, the positioning accuracy in the Asama 2005 survey is better by more than one order of magnitude compared to the 1992 data. Using an up-to-date GPS system, magnetic anomaly changes of several nanotesla would be detectable from repeat aeromagnetic surveys over a volcanic area, where the artificial magnetic disturbance does not reach this threshold.

8. Conclusion

In this study, we applied the generalized mis-tie control method to real data acquired from repeat aeromagnetic surveys over Asama Volcano in order to extract the magnetic anomaly change, and discussed the source of probable errors to evaluate the accuracy of the result. It was evident that simple subtraction of gridded data between magnetic anomalies acquired at two different times is affected by the spatial alias effect, and the generalized mis-tie control method can be successfully applied to reduce this detrimental effect.

The accuracy of magnetic anomaly values was discussed for various error sources. When comparing the 1992 and 2005 survey data of Asama Volcano, it was proven that the positioning inaccuracy of the older 1992 survey was the most serious factor affecting the estimation error of the magnetic anomaly change, because the utilization technique for GPS system had not been sufficiently developed at that time. For the purpose of extracting a magnetic anomaly change by the generalized mis-tie control method, it is especially important to obtain high accuracy positional data. The recent advances in GPS positioning together with precise altimetry techniques would enable us to fly much more accurate reference surveys, and the analysis with the help of the generalized mis-tie control method would enhance the ability of detecting magnetic anomaly change.

From the analysis of aeromagnetic data of Asama Volcano, the magnetic anomaly change exceeding the probable error was detected at three locations. The decrease of the magnetic anomaly value was detected near the summit crater, indicating a loss of magnetization related to the 2004 volcanic activity. Two other locations were characterized by increased anomaly values. A slow process of acquiring stronger magnetization might be in progress in these areas, though we currently do not have any indication of the nature of such a process.

Acknowledgement

The field EM observations including helicopter-borne magnetic survey of Asama Volcano in 2005 was carried out by the Asama Volcano EM Field Experiment Group, consisting of T. Hashimoto, T. Mogi, A. Suzuki, Y. Yamaya (Hokkaido Univ.), M. Mishina (Tohoku Univ.), T. Nakatsuka (AIST), E. Koyama, T. Koyama (Univ. Tokyo), K. Aizawa, J. Hirabayashi, M. Matsuo, K. Nogami, Y. Ogawa, N. Ujihara (Tokyo Inst. Tech.), T. Kagiyama, W. Kanda, A. Okubo, Y. Tanaka, T. Uto, M. Utsugi (Kyoto Univ.), and led by T. Hashimoto. In addition to those included in this paper's authors, E. Koyama, T. Koyama, J. Hirabayashi, T. Kagiyama, W. Kanda, and A. Okubo largely contributed to acquiring the magnetic survey data. We are grateful to all of them for their cooperative work. We are indebted to the Karuizawa Weather Station, Japan Meteorological Agency and Komoro Volcano-Chemical Observatory, Univ. Tokyo for keeping watch on the volcanic activity for the safe field operation under a still active volcanic situation.

We are grateful to the reviewers for their constructive comments and discussion on the manuscript. Especially we are much indebted to Dr. Fausto Ferraccioli for his instructive comments, which were useful to revise and improve the manuscript.

Appendix Original observational data and the process parameters of the data reduction

In the main body, we presented the aeromagnetic anomalies over Asama Volcano in 2005 and in 1992 in the form of those continued to a smooth surface, because the original data at the actual observation height was much influenced by the line-by-line altitude fluctuation. Here we present the original observational data and describe the process parameters used to the data reduction.

Figure A1 illustrates the magnetic anomaly values in the 2005 survey at the actual observation altitude after the diurnal correction and the removal of IGRF-10 field. The distributions between actual survey lines were interpolated without regard to its altitude by the method of "continuous curvature splines in tension" (CCT) developed by Smith and Wessel (1990). The altitude values of the 2005 survey lines are also interpolated by CCT method, as shown in Fig. A2. Similarly, the magnetic anomaly values and the altitudes of the 1992 survey data are illustrated in Figs. A3 and A4. As the magnetic anomaly patterns were much influenced by the observation altitudes, we are going to apply the altitude reduction using the equivalent source technique (Nakatsuka and Okuma, 2006a) to get the magnetic anomaly distribution on a smooth surface. In order to generate a smooth surface to which magnetic anomalies are reduced, 2D weighted average operation was applied to the altitude data, and the altitudes for the 2005 survey shown in Fig. A5 is obtained from the averaging radius of 2 km. This is the reference surface for the magnetic anomaly distribution at the "2005 survey altitude", such as in Figs. 5, 7, etc. Figure A6 shows the reference surface for the magnetic anomaly distribution of the 1992 survey (Fig. 6), obtained from the averaging radius of 1 km. The above-mentioned distributions were calculated at a common grid spacing of 50 m.

In the process of the altitude reduction deriving the magnetic anomaly distribution on a smooth surface, we decided, after several trials, to use the following process parameters. In handling the 2005 data, the equivalent sources were placed with a grid spacing of 50 m on the surface parallel to and 250 m below the smoothed altitude surface (Fig. A5) with a surrounding source (see Nakatsuka and Okuma (2006a)) region of 2 km wide. (The number of unknown parameters amounts to about 70 thousands.) Here the equivalent source quantity is the magnetic anomaly itself, and the kernel function $A(\boldsymbol{p},\boldsymbol{q})$ in Eq. (1) corresponds to the upward continuation operator. Then we solved the inverse problem of Eq. (1) using the conjugate gradient (CG) method. As the method requires an iterative process, we have to terminate it at a certain condition. The process of altitude reduction for the 2005 data was terminated when the misfit improvement became below 1% for consecutive 5 iterations. The final root-mean-square (RMS) misfit was 1.6 nT. Once we obtained the solution for the equivalent sources, it is straightforward to calculate the magnetic anomaly distribution (Fig. 5) on the smooth reduction surface. The 1992 survey data were also processed with a similar condition. Only the difference was that the equivalent source surface was 150 m below the smoothed altitude surface (Fig. A6). However, the situation of convergence in the inversion process was different and there was a large RMS misfit

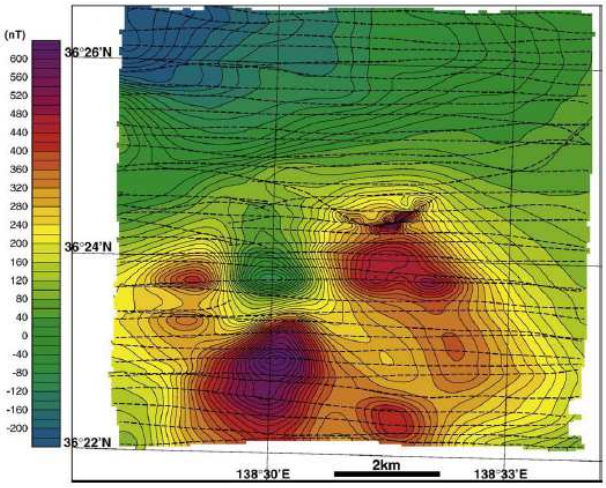

Fig. A1 Magnetic anomaly values at the actual observation altitudes (Fig. A2) in the 2005 survey after the diurnal correction and the removal of IGRF-10 field. Contour interval is 20 nT.

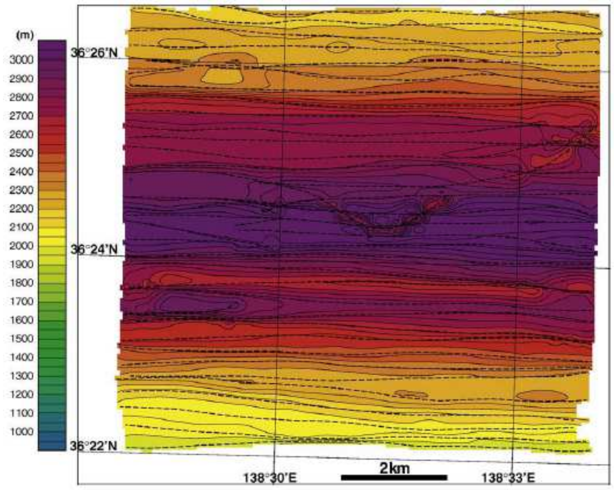

Fig. A2 Altitude values of the actual 2005 survey lines. Contour interval is 50 m.

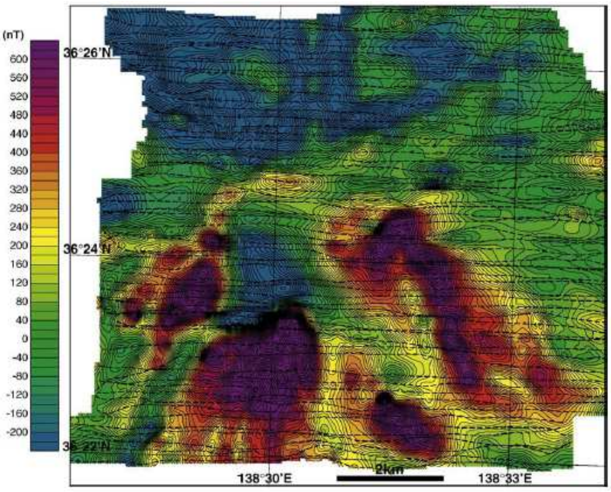

Fig. A3 Magnetic anomaly values at the actual observation altitudes (Fig. A4) in the 1992 survey after the diurnal correction and the removal of IGRF-10 field. Contour interval is 20 nT.

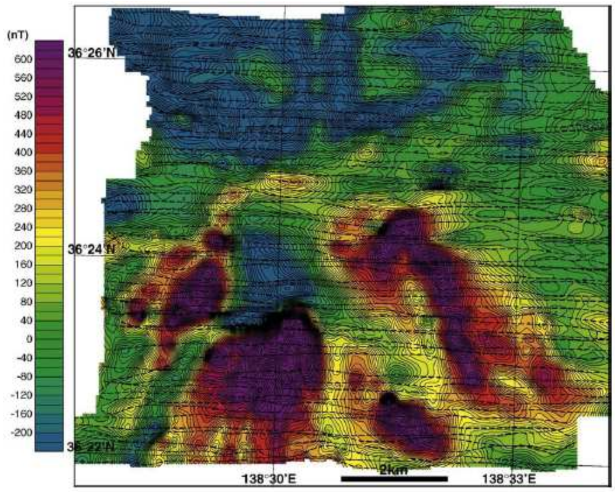

Fig. A4 Altitude values of the actual 1992 survey lines. Contour interval is 50 m.

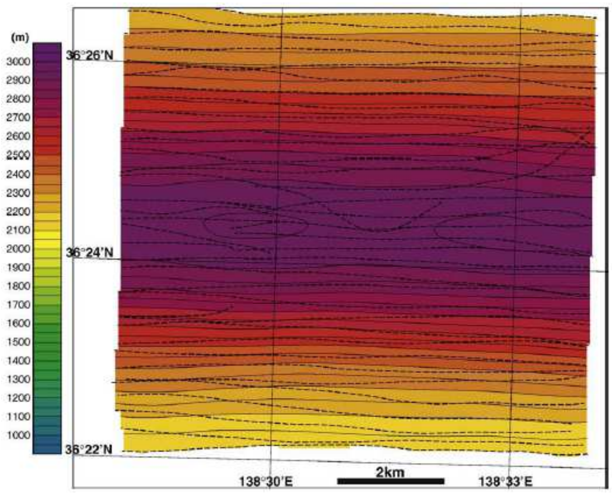

Fig. A5 Smooth reference surface (2005) to which the magnetic anomalies in Fig. 5 were reduced. Contour interval is 50 m.

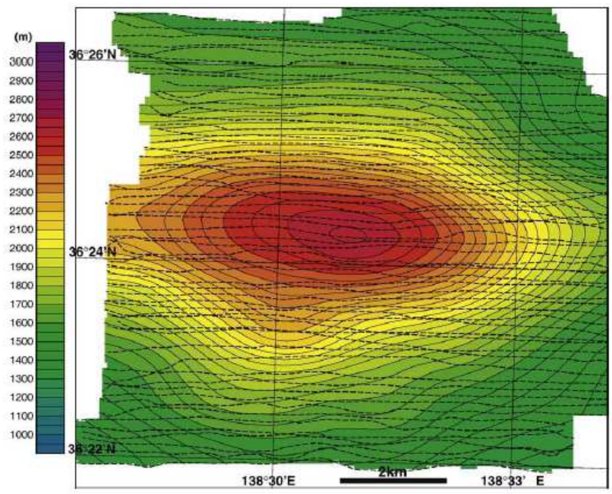

Fig. A6 Smooth reference surface (1992) to which the magnetic anomalies in Fig. 6 were reduced. Contour interval is 50 m.

of 15 nT when the misfit improvement became below 1% for consecutive 5 iterations. Therefore, we continued the iteration until the RMS misfit became less than 5 nT. This poorer convergence probably came from the inaccuracy of positioning data of the 1992 survey. Nevertheless, the error effect on the result of the generalized mis-tie control method is much smaller, as the temporal magnetic anomaly change is evaluated at the higher altitudes of the 2005 survey. For example, two reductions to the surface of the 2005 survey (Fig. A5) from the intermediate equivalent source model with a RMS misfit of 15 nT and from the final one with 5 nT misfit revealed better coincidence with a RMS difference of 4.4 nT.

The generalized mis-tie control method (Nakatsuka and Okuma, 2006b) has a character that it is an extension of the altitude reduction by equivalent sources, and the process parameters are common to both processes, except that the generalized mis-tie control method requires another parameters, the locations of the control points. Also there are so many similar processes utilized in the body discussion. But it will be of no use to describe all the parameters of them. We only mention that we used almost the same configuration with a common grid spacing of 50 m in the data analysis.

References

Aramaki, S., 1993, Geological map of Asama Volcano (1:50,000), *Geological Maps of Volcanoes*, no. 6, Geological Survey of Japan.

Hamano, Y., H. Utada, T. Shimomura, Y. Tanaka, Y. Sasai, I. Nakagawa, Y. Yokoyama, M. Ohno, T. Yoshino, S. Koyama, T. Yukutake, and H. Watanabe, 1990, Geomagnetic variations observed after the 1986 eruption of Izu-Oshima volcano, *J. Geomag. Geoelectr.*, **42**, 319-335.

Hashimoto, T., 2006, Apparent total field change due to secular variation −evaluation of volcanomagnetic effect−, *2006 Proc. Conductivity Anomaly Research*, 51-58. (in Japanese with English abstract)

Hurst, A. W., P. C. Rickerby, B. J. Scott, and T. Hashimoto, 2004, Magnetic field changes on White Island, and the value of magnetic changes for eruption forecasting, *J. Volcanol. Geotherm. Res.*, **136**, 53-70.
doi: 10.1016/j.jvolgeores.2004.03.017

Maus, S. and S. Macmillan, 2005, 10th Generation International Geomagnetic Reference Field, *EOS, Trans. AGU*, **86** (16), 159. doi: 10.1029/2005EO160006

Nagata, T., 1943, The natural remanent magnetism of volcanic rocks and its relation to geomagnetic phenomena, *Bull. Earthq. Res. Inst., Tokyo Imp. Univ.*, **21**, 1-196.

Nagata, T. and S. Uyeda, 1961, Thermo-remanent magnetization, *in* T. Nagata (ed.), *Rock magnetism*, 147-195, Maruzen, Tokyo.

Nakatsuka, T., M. Makino, S. Okuma, and T. Kaneko, 1990, Aeromagnetic surveys over Izu-Oshima volcano before and soon after the 1986 eruption, *J. Geomag. Geoelectr.*, **42**, 337-353.

Nakatsuka, T., 1994, Aeromagnetic anomalies over the area of Unzendake Volcano, *J. Geomag. Geoelectr.*, **46**, 529-540.

Nakatsuka, T., 1995, Minimum norm inversion of magnetic anomalies with application to aeromagnetic data in the Tanna area, Central Japan, *J. Geomag. Geoelectr.*, **47**, 295-311.

Nakatsuka, T., and S. Okuma, 2006a, Reduction of geomagnetic anomaly observations from helicopter surveys at varying elevations, *Explor. Geophys.*, **37**, 121-128.
doi: 10.1071/EG06121

Nakatsuka, T., and S. Okuma, 2006b, Crossover analysis for the aeromagnetic survey at varying elevations, and its application to extracting temporal magnetic anomaly change, *Butsuri-Tansa (Geophys. Explor.)*, **59**, 449-458.

Okuma, S., T. Nakatsuka, R. Morijiri, M. Makino, T. Uchida, Y. Ogawa, S. Takakura, and N. Matsushima, 2001, Preliminary results of a high-resolution aeromagnetic survey over Usu Volcano, Hokkaido, Japan. *Bull. Geol. Surv. Japan*, **52**, 149-154. (in Japanese with English abstract)

Okuma, S., T. Nakatsuka, R. Morijiri, and M. Makino, 2003, High-resolution aeromagnetic anomaly map of Usu Volcano (1:25,000). *Total Intensity Aeromagnetic Maps*, no.41, Geol. Surv. Japan, AIST.

Okuma, S., M. Makino, and T. Nakatsuka, 2005, High-resolution aeromagnetic anomaly map of Asama Volcano (1:25,000). *Total Intensity Aeromagnetic Maps*, no.43, Geol. Surv. Japan, AIST.

Rikitake, T. and I. Yokoyama, 1955, Volcanic activity and changes in geomagnetism, *J. Geophys. Res.*, **60**, 165-172.
doi: 10.1029/JZ060i002p00165

Sasai,Y., M. Uyeshima, J. Zlotnicki, H. Utada, T. Kagiyama, T. Hashimoto, and Y. Takahashi, 2002, Magnetic and electric field observations during the 2000 activity of Miyake-jima volcano, Central Japan, *Earth Planet. Sci. Lett.*, **203**, 769-777. doi: 10.1016/S0012-821X(02)00857-9

Smith, W. H. F., and Wessel, P., 1990, Gridding with continuous curvature splines in tension, *Geophysics*, **55**, 293–305. doi: 10.1190/1.1442837

Tanaka, Y., 1993, Eruption mechanism as inferred from geomagnetic changes with special attention to the 1989-1990 activity of Aso Volcano, *J. Volcanol. Geotherm. Res.*, **56**, 319-338. doi: 10.1016/0377-0273(93)90024-L

Ueda, Y., 2006, 3D magnetic structure of Miyake-jima Volcano before and after the eruption in 2000, *Bull. Volc. Soc. Japan*, **51**, 161-174. (in Japanese with English abstract)

Ueki, S., S. Okubo, H. Oshima, T. Maekawa, W. Sun, S. Matsumoto, and E. Koyama, 2005, Gravity change preceding the 2004 eruption of Asama Volcano, Central Japan, *Bull. Volc. Soc. Japan*, **50**, 377-386. (in Japanese with English abstract)